Cell Cycle

ISSN: 1538-4101 (Print) 1551-4005 (Online) Journal homepage: http://www.tandfonline.com/loi/kccy20

ZFP36 expression impairs glioblastoma cell lines viability and invasiveness by targeting multiple signal transduction pathways

Tommaso Selmi, Andrea Martello, Tatiana Vignudelli, Erika Ferrari, Alexis Grande, Claudia Gemelli, Paolo Salomoni, Sergio Ferrari & Tommaso Zanocco-Marani

To cite this article: Tommaso Selmi, Andrea Martello, Tatiana Vignudelli, Erika Ferrari, Alexis Grande, Claudia Gemelli, Paolo Salomoni, Sergio Ferrari & Tommaso Zanocco-Marani (2012) ZFP36 expression impairs glioblastoma cell lines viability and invasiveness by targeting multiple signal transduction pathways, Cell Cycle, 11:10, 1977-1987, DOI: 10.4161/cc.20309

To link to this article: http://dx.doi.org/10.4161/cc.20309

Published online: 15 May 2012.

Cell Cycle 11:10, 1977-1987; May 15, 2012; © 2012 Landes Bioscience

ZFP36 expression impairs glioblastoma cell lines viability and invasiveness by targeting multiple signal transduction pathways

Tommaso Selmi,[1,3] Andrea Martello,[1] Tatiana Vignudelli,[1] Erika Ferrari,[2] Alexis Grande,[1] Claudia Gemelli,[1] Paolo Salomoni,[3] Sergio Ferrari[1] and Tommaso Zanocco-Marani[1,*]

[1]Dipartimento di Scienze Biomediche; Sezione di Chimica Biologica; Università di Modena e Reggio Emilia; Modena, Italy; [2]Dipartimento di Chimica; Università di Modena e Reggio Emilia; Modena, Italy; [3]Samantha Dickson Brain Cancer Unit; UCL Cancer Institute; London, UK

Key words: glioblastoma, ZFP36, PIM kinases, XIAP, cell death, ripoptosome, tristetraprolin, TTP

Abbreviations: TTP, tristetraprolin; ZFP36, zinc finger protein 36 homolog; ARE, AU-rich elements; UTR, untraslated region; RP, reverse primer; DP, direct primer; E.V., empty vector; Ctr, control; C.E., cinnamon extracts

RNA binding proteins belonging to the TIS11/TTP gene family regulate the stability of multiple targets. Their inactivation or deregulated expression has recently been related to cancer, and it has been suggested that they are capable of displaying tumor suppressor activities. Here we describe three new targets of ZFP36 (PIM-1, PIM-3 and XIAP) and show by different approaches that its ectopic expression is capable of impairing glioblastoma cell lines viability and invasiveness by interfering with different transduction pathways. Moreover, we provide evidence that compounds capable of inducing the expression of TIS11/TTP genes determine a comparable biological effect on the same cell contexts.

Introduction

The TTP family of tandem zinc finger proteins includes TTP/ZFP36, TIS11b/ZFP36L1 and TIS11d/ZFP36L2, all of which have been shown to directly bind AU-rich elements (ARE) and promote degradation of the host transcript.[1,2] Their central RNA-binding domain interacts with AU-rich elements (UUA UUU AUU), whereas the N- and C-terminal domains recruit enzymes involved in the mRNA degradation pathway. Expression of all TTP family members genes can be induced by various mitogenic stimuli, such as growth factors, in a broad variety of cell types.[3,4] For instance, it has been demonstrated that ZFP36 binds to and destabilizes the TNFα, GM-CSF and VEGF mRNAs.[1,5,6] This, in turn, affects the function of transcription factors such as NFκB and HIF-1, which have an important impact on cell viability.[7,8] Several publications demonstrate that TTP family proteins are phosphorylated[9] and are possible targets along the p38 MAPK pathway.[10,11] At the biological level, TTP family members have been described as involved in cell differentiation and apoptosis,[12,13] in the regulation of the cell response to growth factors and in the development of cancer. In particular, it has been demonstrated that TTP proteins target and destabilize mRNAs encoding growth factors' signaling transducers, particularly downstream of EGF[14] and IGF-I receptors.[4] Moreover, it has been recently suggested that members of this family are also capable of acting by ARE-mediated decay-independent mechanisms. For instance ZFP36 is able to terminate NFκB signaling by directly interfering with the nuclear import of the p65 subunit of the transcription factor.[15] As regards cancer biology, it has been shown that ZFP36 may alter the tumorigenic phenotype and patient prognosis,[16] probably targeting several oncogenes. ZFP36 is downregulated in many cancers, and, in particular, it has been shown that ZFP36 is hyperphosphorylated and therefore inactive in gliomas,[17] this leading to stabilization of VEGF and IL-8 mRNAs.

Glioblastoma multiforme (GBM) is the most common and malignant subset of brain tumors; thus, understanding the mechanisms mediating cellular survival and apoptosis resistance will enable to design smarter drug combinations in targeted cancer therapies. GBMs have been traditionally defined as two clinically and cytogenetically distinct diseases, the primary or de novo vs. the secondary GBMs. The latter classically afflict younger persons (median age ~45 y) and evolve from the slow progression (mean, 4–5 y) of a low-grade glioma, which usually displays aberrations in platelet-derived growth factor receptor (PDGFR) and Tp53 genes. Primary GBMs present acutely as a high-grade disease that most frequently affects the elderly. They typically harbor mutations in epidermal growth factor receptor (EGFR), cyclin-dependent kinase inhibitor 2A (CDKN2A) and loss of heterozygosity (LOH) on chromosome 10q23, which houses the phosphatase and tensin homolog (PTEN) gene. LOH on chromosome 10 is the most frequent genetic alteration in primary

*Correspondence to: Tommaso Zanocco-Marani; Email: zanocco@unimore.it
Submitted: 02/27/12; Revised: 04/05/12; Accepted: 04/09/12
http://dx.doi.org/10.4161/cc.20309

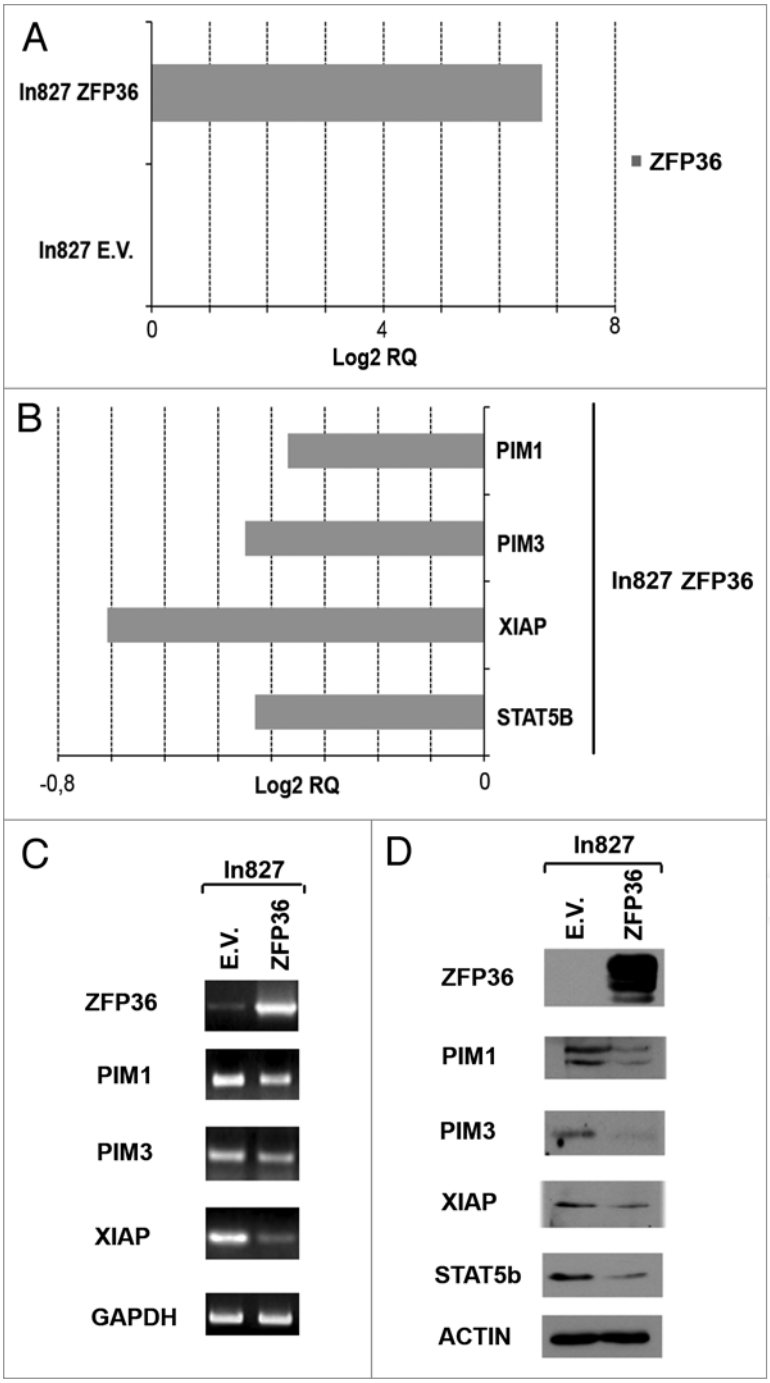

Figure 1. Overexpression of ZFP36 in the ln827 glioma cell line triggers the degradation of the oncogenic kinases PIM1, PIM3 and of the X-linked inhibitor of apoptosis (XIAP) mRNAs. (A) The overexpression levels of ZFP36 in ln827 were assessed by quantitative real-time PCR (QRT-PCR). (B) Following ZFP36 overexpression, the mRNAs of PIM1, PIM3 and XIAP are down-modulated. QRT-PCR data are expressed as Log2 of relative quantity compared with the expression levels of the same genes in ln827 cells transfected with empty vector. Stat5b has been used as a positive control for ZFP36 activity. (C and D) ln827 cell line expresses high levels of PIM1, PIM3 and XIAP. (C) RT-PCR confirms the negative regulation exerted by exogenous ZFP36 on the mRNAs of the targets described in this study. (D) In line with the decrease in the mRNA levels, western blots following ZFP36 transduction show a drop in protein levels of PIM1, PIM3, XIAP and Stat5b compared with the E.V. population. All samples were collected 48 h after transfection with pcDNA3.1 ZFP36/pcDNA3.1 E.V.

GBMs, occurring in 60–80% of cases.[18] Mutations in the EGF receptor result in ligand-independent constitutive tyrosine kinase activity that activates persistent downstream RAS/RAF/MAPK growth and PI3K survival signaling.[19] As regards the invasion potential of glioblastomas, extensive studies show that STAT3 (through JAK/Stat pathway) and NFκB transcription factors support migratory and invasive potential of glioblastoma cells.[20,21] In particular, constitutive NFκB activity positively regulates the expression of VEGF and IL-8 and tumor angiogenesis of human glioblastoma.[22] Although much is known about the diverse genotypes causing the heterogeneous histological phenotypes of GBMs and how they impact on survival signaling, there is still no therapy that induces tumor cell apoptosis beyond that of the standard treatment. Several studies on GBM clearly demonstrate that targeting of IAPs (inhibitor of apoptosis proteins) sensitizes cells to apoptosis,[23] and a recent report showed that XIAP inhibitors synergize with radiation to increase glioblastoma cell apoptosis.[24,25] Furthermore, targeting of IAPs also increases sensitivity to TRAIL-induced apoptosis, and IAPs' depletion induces the assembly of the "ripoptosome," thereby triggering cell death.[26] Interestingly, several players in the GBM tumor paradigm, such as VEGF, IL-8, NFκB and STAT5b, have already been described as direct targets of TTP genes, while others, such as STAT3, PIM1, PIM3 and XIAP, are considered putative ones, since they carry AU-rich elements in their mRNAs' 3'-UTR. This observation suggests that, by acting on the expression of TTP genes, it might be possible to impinge on GBM growth, viability and chemoresistance by determining the downregulation of several oncogenes.

Results

ZFP36 ectopic expression interferes with endogenous levels of XIAP, PIM1 and PIM3 in the GBM cell line ln827. Ln827 cells express very low levels of ZFP36 and were the main tool used for ectopic expression assays. **Figure 1A–D** shows the effect of ZFP36 ectopic expression on its putative target genes XIAP, PIM1 and PIM3. In particular, (A) shows a QRT-PCR measuring the ectopic expression of ZFP36 obtained on ln827 cells compared with the empty vector-treated population (ln827E.V.). (B) is a QRT-PCR performed on the same cell populations showing that ln827-ZFP36 cells display lower levels of XIAP, PIM1, PIM3 and Stat5b expression compared with the control population ln827E.V. The analysis of Stat5b expression was included as a control of ZFP36 activity, since in a previous work it was demonstrated that Stat5b is a target of ZFP36.[27] (C and D) show the same results obtained by different techniques. In particular, (C) shows a semi quantitative RT-PCR, and (D) depicts different western blots

showing that, following ZFP36 ectopic expression, a decrease in the expression of PIM1, PIM3, XIAP and Stat5b occurs also at the protein level. As a whole, the inverse correlation between the expression of PIM1, PIM3, XIAP and ZFP36 together with the presence of AREII sequences in their 3' untranslated regions (3' UTR) strongly suggests that such genes are indeed ZFP36 direct targets.

ZFP36L1 directly binds PIM1, PIM3 and XIAP 3' UTRs and thereby affects their stability. Since PIM1, PIM3 and XIAP carry AREII-like nonameres in their 3' UTR regions, to demonstrate that they are directly targeted by ZFP36, we performed a luciferase reporter assay, generating luciferase reporter constructs (pGL3-based) allowing transcription of a luciferase mRNA carrying the 3' UTRs of PIM1, PIM3 or XIAP. The results are shown in **Figure 2**. (A) shows that co-expression of the reporter vector encoding PIM1 3' UTR with a vector expressing ZFP36 significantly decreases the basal reporter activity, demonstrating that by directly binding the described mRNA, ZFP36 impairs protein production by either promoting mRNA degradation or by inhibiting mRNA translation. (B and C) represent the same kind of experiment performed by co-expressing ZFP36 with the reporter vectors carrying the 3' UTR of PIM3 and XIAP, respectively. Again, the assay shows that ZFP36 is capable of directly binding and therefore destabilizing the mRNAs of PIM3 and XIAP.

ZFP36 ectopic expression impairs colony formation of ln827 cells. To evaluate if, by restoring ZFP36 expression, it is possible to impinge on the malignancy of GBM cells, we performed a soft agar assay on ln827 cells overexpressing ZFP36 (ln827 ZFP36) and compared them to an empty vector-treated sample (ln827E.V.). The results of such experiment are shown in **Figure 3**. (A) shows two pictures suggesting that in the population overexpressing ZFP36, colonies are not only less numerous, but also considerably smaller. (B) summarizes a series of experiments demonstrating that ZFP36 expression determines a consistent reduction of 30% of colonies compared with the control cell population. Since we hypothesized that the anti-proliferative or death-inducing effect of ZFP36 might reside in its capability to downregulate the expression of target genes such as PIM1, PIM3 and XIAP, we performed soft agar assays on ln827 cells in which these genes were silenced and compared them to ln827 cells treated with a control siRNA (ctr siRNA). The results of such experiment are described in **Figure 3C and D**. PIM1, PIM3 and XIAP were silenced singularly or at the same time. (C) represents a QRT-PCR describing the efficacy of the silencing treatments in the different populations, while (D) shows the numbers of colonies in different sets of experiments. As it was expected, by silencing PIM1, PIM3 and XIAP, a decrease in the number of colonies is observed by soft agar assay, and, interestingly, the cumulative silencing determines the strongest impairment of colony formation.

The decreased colony formation depends on cell death rather than on slower proliferation. To evaluate whether the lower number of colonies observed in the previous assays depends on increased cell death or on a lower proliferation

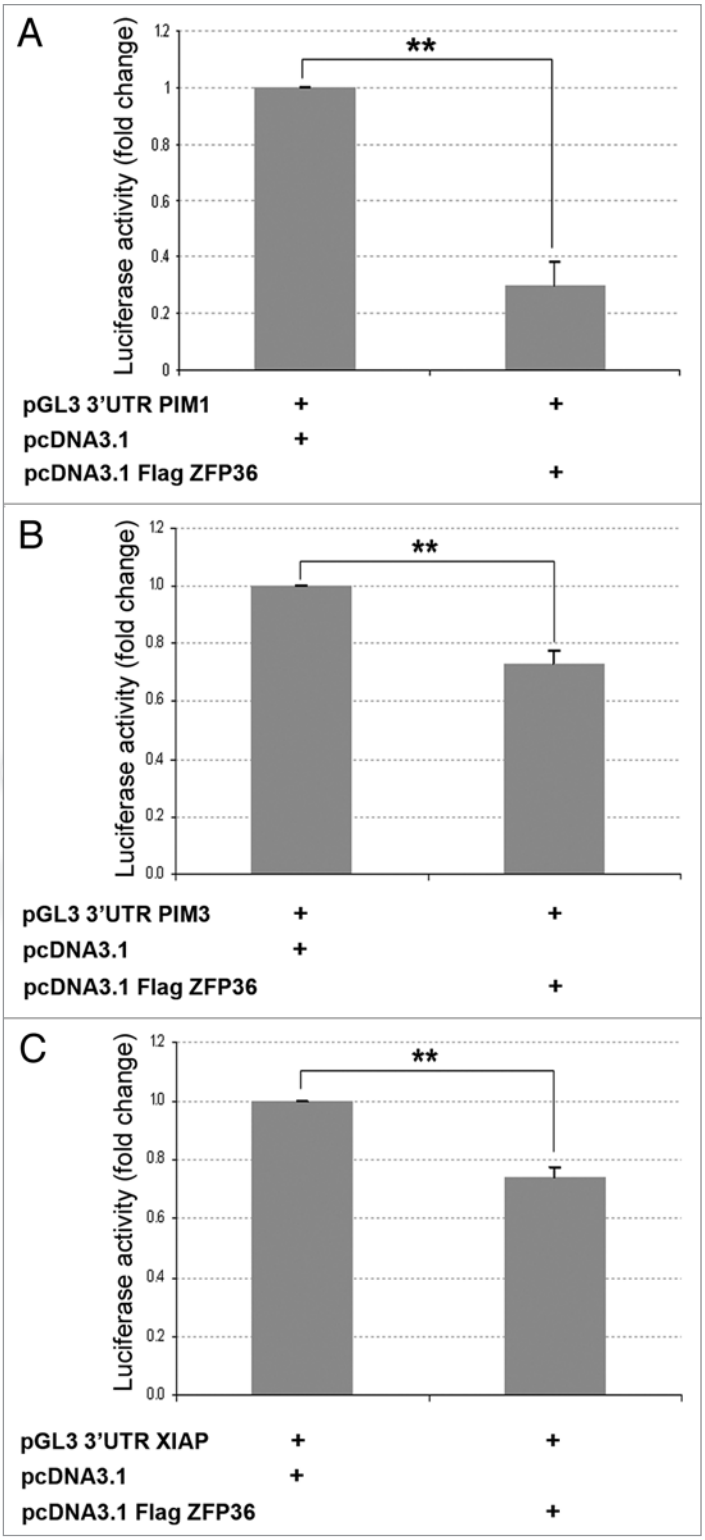

Figure 2. (A) Luciferase activity assays showing that ZFP36 induces decreased expression of mRNAs carrying the 3′ UTR of PIM1, PIM3 or XIAP. (A) Luciferase activity was assayed in HEK293 cells transfected with empty pcDNA3.1 vector or with pcDNA3.1 vector expressing FlagZFP36 (10 ng) together with pGL3 reporter construct encoding for a luciferase gene fused to the 3′ UTR of PIM1. Similar experiments were performed with pcDNA3.1 vector expressing FlagZFP36 together with pGL3 reporter construct encoding for a luciferase gene fused to the 3′ UTR of PIM3 (B) or XIAP (C). Data represent mean and SEM for n = 4, **p < 0.01.

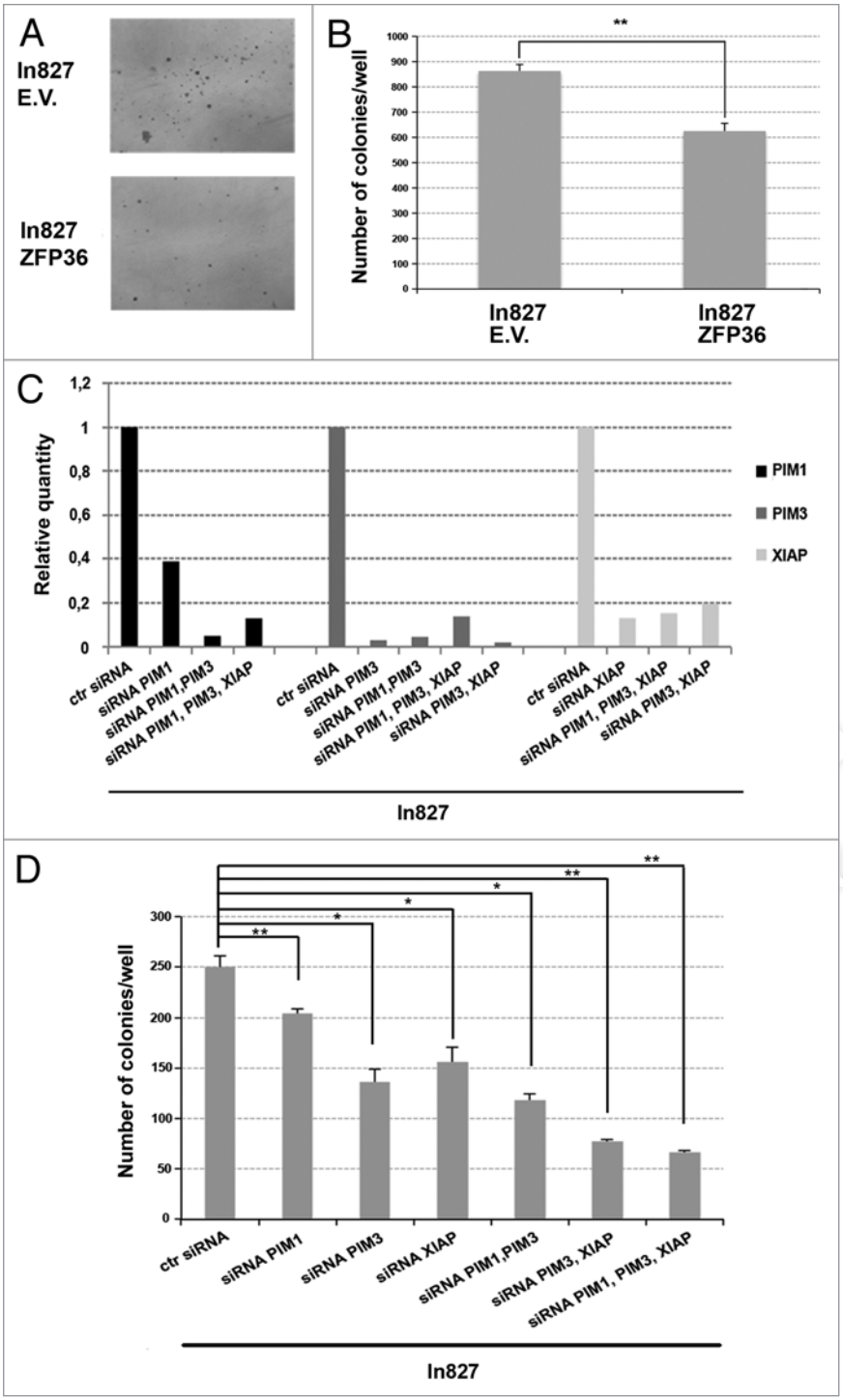

Figure 3. (A and B) Effect of ZFP36 overexpression on anchorage independent growth in ln827. After infection and selection for stable transduction, pBABE E.V. and pBABE ZFP36 cells were plated in soft agar. After 21 d colonies were scored. (A) 5x magnification phase contrast picture shows the morphology of the scored colonies for each sample. ZFP36 expression induces a strong reduction in size of the grown colonies when compared with the empty vector population. (B) ZFP36 expression also impairs the anchorage-independent growth of ln827, as demonstrated by the number of scored colonies, which is consistently lower in the ZFP36 population. (C and D) Anchorage-independent growth of ln827 relies on the expression of PIM1, PIM3 and XIAP. (C) QRT-PCR is representative of the efficacy of gene silencing achieved in ln827 through pooled oligo siRNAs transfection. Control siRNA population was set as calibrator in each experiment. (D) siRNA-transfected cells were plated in soft agar 72 h after transfection then scored 14 d later. As shown in (D), single silencing of PIM1, PIM3 or XIAP impairs the colony formation ability of ln827. The concurrent silencing of these genes has a cumulative effect that strongly counteracts the colony formation. The bars in (B and D) represent SEM for three independent experiments, *p < 0.05, **p < 0.01.

rate, we performed cell cycle analysis and growth curves (data not shown) suggesting that it is not an impairment of proliferation underlying the low number of colonies formed by ln827 cells ectopically expressing ZFP36. Successively, we evaluated by different techniques the viability of the different cell populations. Results of such analysis are summarized in **Figures 4 and 5**. In the first experiment (**Fig. 4**), we performed a count of condensed nuclei, shown in (A), to generally evaluate the number of cells supposedly undergoing apoptosis. As far as ln827 cells overexpressing ZFP36 are concerned, data are shown in (B), showing that the percentage of condensed nuclei is consistently 20% higher in ln827 ZFP36 compared with ln827E.V. To complete this set of data, we counted nuclei in ln827 cells that previously underwent silencing of PIM1, PIM3 and XIAP. Results are given in (C) and show that, in accord with soft agar results, the highest death rates are obtained when the target genes are inactivated simultaneously, and it has to be underlined that the downregulation of PIM3 and XIAP seems to be particularly relevant in order to induce cell death.

To assess if the observed death depends on apoptosis, we performed a TUNEL assay on ln827 ZFP36 cells and successively an annexin V/PI assay. Results are shown in **Figure 5**. (A) is an immunofluorescence staining of ZFP36 coupled to the TUNEL assay. Interestingly, a small amount of DNA fragmentation is visible only in cells ectopically expressing ZFP36. To better elucidate the type of cell death, a double staining annexin V-propidium iodide was performed. Results shown in **Figure 5B and C** were obtained at time points of 24 and 48 h after infection. (B) shows that ln827 ZFP36 cells display significantly higher levels of both annexin V and PI positivity compared with the control population ln827E.V. Nevertheless, we were not able to identify any Annexin V single-positive population at any time point (data not shown), suggesting that the cell death triggered by ZFP36 involves a program which is different from classical apoptosis. We monitored to see if comparable results could be obtained by silencing PIM1, PIM3 and XIAP in

ln827 cells. Data are shown in (C), where the mutual gene silencing of the target genes induces high positivity to annexin V/PI.

Since CASP3 activity was not detected following ZFP36 ectopic expression (data not shown), we hypothesized that XIAP's depletion determined by ZFP36 could lead to ripoptosome's aggregation[26] and subsequent death via CASP8 activation. To verify this hypothesis, we performed an immunoblot (**Fig. 5D**) showing that following ZFP36 ectopic expression, ln827 cells display RIPK1 stabilization and CASP8 activation represented by the appearance of low molecular weight forms and by a decrease in intensity of the high molecular weight un-cleaved form. Interestingly, we were also able to detect by western blot an increase of a peculiar form of cleaved PARP-1 (**Fig. 5E**), characterized by the appearance of 116, 55 and 42 KDa bands, compatible with the programmed necrotic cell death.[38]

Ectopic expression of ZFP36 reduces the invasion ability of ln827 cells. Since published data suggest that inhibition of Stat5b reduces the invasion potential of human GBM cells,[29] and that PIM3 kinase inhibitors downregulate STAT3(Tyr705) phosphorylation,[30] thereby impinging on the ability of Stat3 to promote invasion,[31,32] we evaluated whether ectopic expression of ZFP36 is capable of reducing invasion by inducing the downregulation of Stat5b and PIM3 simultaneously. To collect evidences to this regard, we performed wound-healing assays on ln827 ZFP36 and compared them to ln827E.V. The results are shown in **Figure 6A**, where 72 h after the wound was inflicted, ln827 ZFP36 do not display the same capability to fill the gap as ln827E.V. To demonstrate that the observed impairment in the invasiveness relies on the inactivation of specific targets, we performed other wound-healing assays, shown in **Figure 6B**, on ln827 cells in which PIM3/XIAP or PIM3/PIM1/XIAP were silenced and compared their invasion potential to ln827 treated with a control siRNA. As expected, the populations where PIM1, PIM3 and XIAP were silenced did not show, after 72 h, the same ability of the control population to repair the wound, although at a lower extent compared with ZFP36 overexpression, suggesting that other targets might be involved in the inhibition of wound repairing.

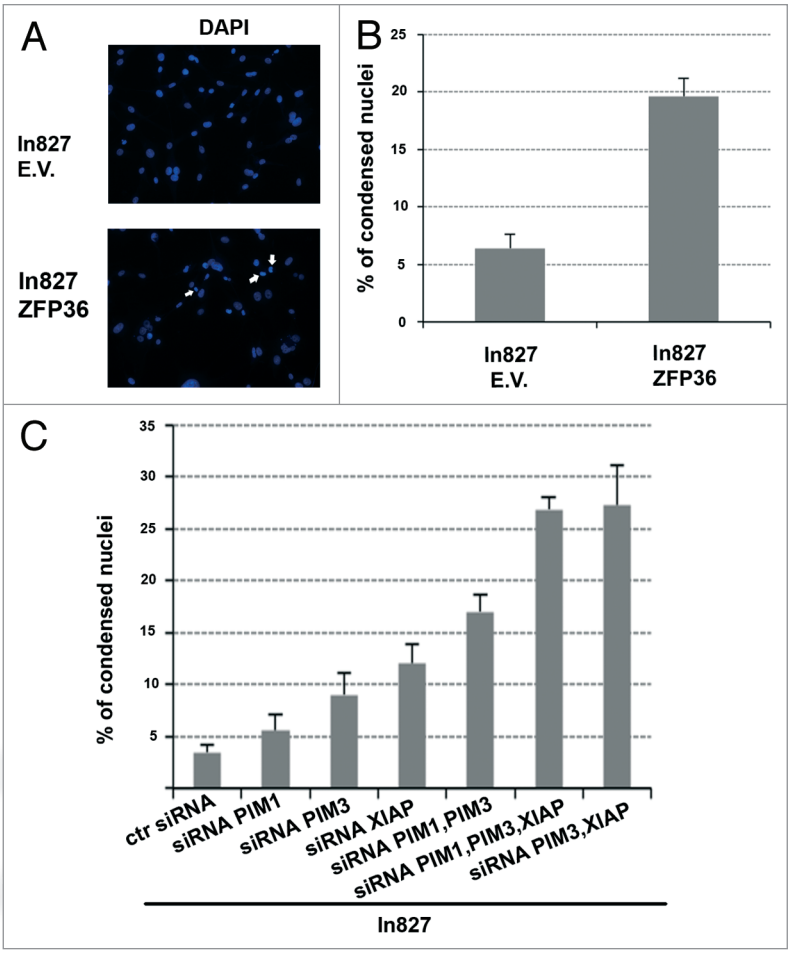

Figure 4. Condensed nuclei evaluation in ln827E.V./ZFP36 and in ln827 after PIM1, PIM3 and XIAP depletion by oligo siRNA strategy. (A) DAPI staining of pBABE ZFP36 and pBABE E.V. ln827. Cells that undergo ZFP36 overexpression show higher number of both condensed nuclei and micronuclei when compared with the E.V. population. (B) ZFP36 population is characterized by a higher frequency of nuclear condensation when compared with the E.V. population. (C) Gene silencing by pooled oligo siRNAs of PIM1, PIM3, XIAP reproduces the effect of ZFP36 expression. Again, the multiple silencing of these genes shows to be more effective than the single targeting strategy. The graphs in this figure represent the mean and SEM of n = 3 experiments, in each of which ten fields were scored for each cell population. The number of condensed nuclei over the total number of nuclei gives the percentage shown by the graphs.

Cinnamon polyphenols induce cell death of ln827 cells. To further verify the data collected so far, it was elected to test the biological effect of cinnamon extracts (C.E.), compounds capable of inducing the expression of ZFP36 and other members of the same gene family[27,33] on ln827 cells. The data are described in **Figure 7**. (A) represents a QRT-PCR showing that C.E. induces the expression of ZFP36. In (B), pictures are shown that demonstrate a change in the morphology of ln827 cells treated with C.E. that, following the treatment, detach from the plate. Coupled to the morphological pictures, (B) also carries the DAPI staining of the nuclei clearly showing that condensed apoptotic nuclei are largely represented in the treated population. To confirm the fact that compounds capable of inducing the expression of ZFP36 push ln827 cells toward apoptosis, we performed a cell cycle analysis. The result of this last assay is shown in **Figure 7C**, where in the part representing ln827C.E., a clear sub-G_1 peak appears, further suggesting that the analyzed population is undergoing cell death.

Discussion

Although it was originally described as an important regulator of the inflammatory response, a growing body of publications shows that ZFP36 is deficient in cancer cells when compared with normal cell types,[16] and that its expression counteracts malignant progression by interfering with different pathways, depending on the disease model.[34-37]

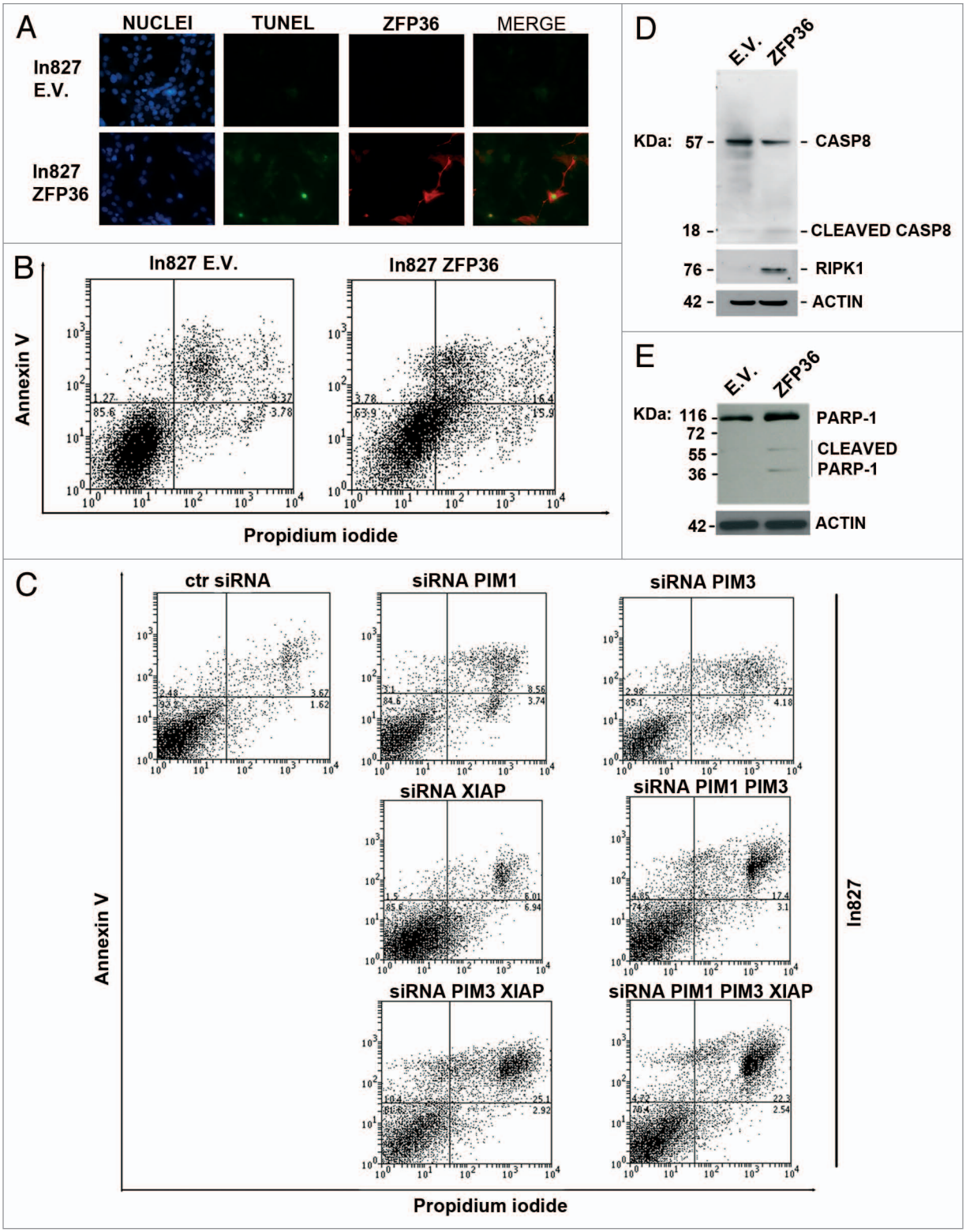

Figure 5. For figure legend, see page 1983.

The fact that ZFP36 and the other members of this gene family, such as ZFP36L1, are capable of inducing the degradation of quite a large number of mRNAs, among whom are listed those encoding several oncogenes, explains why their targeting seems to be effective in very different and heterogeneous disease models. For this reason, we decided to verify the activity of ZFP36 in GBM cell lines.

GBM is genetically highly heterogeneous, and it still has a negative outcome, since no effective therapy has been established.

Figure 5 (See opposite page). ZFP36-mediated inhibition of PIM1, PIM3 and XIAP induces cell death of glioma cells. (A) Transfected ln827 cells were plated on coverslips, and 48 h after transfection, they were subjected to TUNEL assay. Positive staining is detected only in the ZFP36-expressing population. (B) Cell death was measured at different time points after transduction as the proportion of cells positive for Annexin V and propidium iodide. Annexin V values are graphed on the y axis, while PI values are on the x axis. The numbers in the lower right corners represent the percentage of positive cells. Ln827 ZFP36 show increased percentage of both AnnexinV/PI double positive and PI single positive cells. (C) Oligo siRNA transfection of the glioma cell line was performed as described and apoptosis was assessed by Annexin V/PI staining. The single silencing of PIM1, PIM3 and XIAP induces positivity to the apoptotic markers but is less efficient than the simultaneous multiple gene silencing, which strongly increases the percentage of the Annexin V/PI double positive population. (D) Western blot analysis shows caspase 8 cleavage and concomitant increase of the RIP1 kinase upon ZFP36 expression. (E) Western blot analysis of PARP-1 shows the appearance of 55 KDa and 42 KDa bands in the ln827 ZFP36 population.

Moreover, there is evidence suggesting that ZFP36 is inactivated in gliomas,[17] and we collected further evidence (**Fig. 1A**) that in ln827 GBM cell lines, ZFP36 is expressed at very low levels.

Another aspect strengthening the hypothesis that targeting ZFP36 could impinge on GBM biology, resides on published data suggesting that ZFP36 negatively regulates EGFr pathway,[14] which is particularly important during the development of the disease, and that among its targets there's also Stat5b,[27] whose activity participates in determining the proliferative activity and the invasion capability of GBM cells.[29] To verify the effect of ZFP36 expression on GBM cells, we performed ectopic expression experiments and, while doing so, we demonstrated that the kinases PIM1 and PIM3 and X-linked inhibitor of apoptosis protein (XIAP) are new ZFP36 targets.

PIM family's serine/threonine kinases play an important role in cancer biology. Whereas elevated levels of PIM1 and PIM2 are mostly found in hematologic malignancies and prostate cancer, increased PIM3 expression is observed in different solid tumors.[38] PIM1 and PIM3 are active as oncogenes when their expression increases, owing to a loss of regulation; therefore, it was reasonable to think that by inducing the expression of a gene capable of determining their downregulation, ZFP36, by the hypothesis, would be possible to counteract their oncogenic activity. Among other activities, PIM1 and PIM3 act by repressing apoptosis[30,39,40] and by stimulating the invasion activity of cancer cells.[41] These characteristics are reflected in the gene silencing experiments shown here, where downregulation of PIM1 and PIM3 expression determines cell death and a decrease of invasiveness. In particular, as far as GBM cells are concerned, PIM3 seems to be more relevant than PIM1.

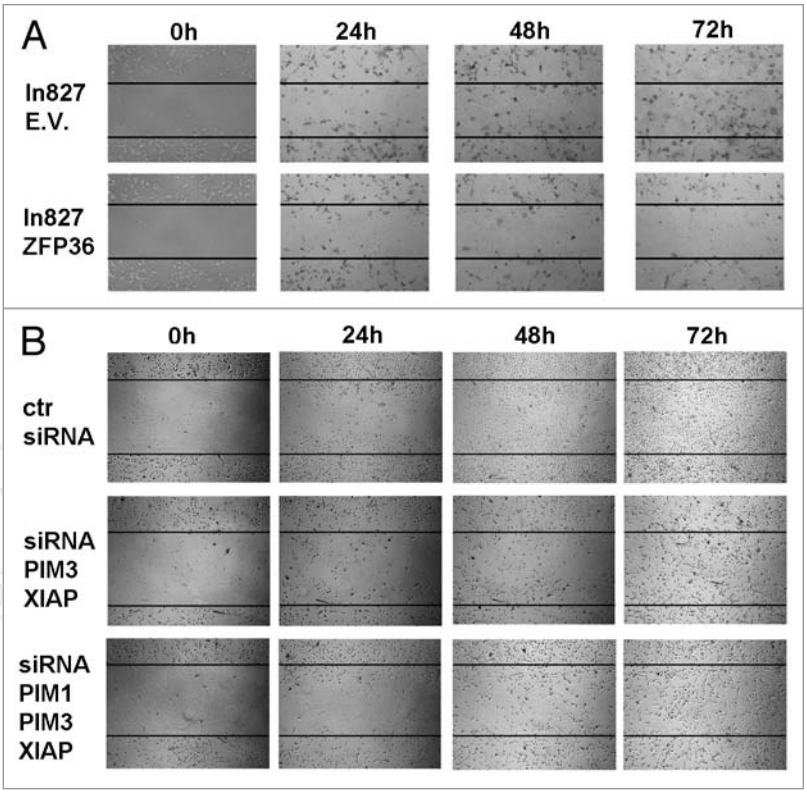

Figure 6. Migration of glioma cells is inhibited by ZFP36 through downregulation of PIM3 and XIAP. (A and B) Wound-healing assay was performed as described and cells were checked every 24 h. Similar results were obtained in three independent experiments. ZFP36 expressing cells show a relevant impairment of their migration potential. Silencing of PIM3 and XIAP partially recapitulates this effect.

XIAP is a E3 ubiquitine ligase, member of the IAP family, whose other member cIAP2 had already been characterized as a target of ZFP36.[42] Although it is clear that IAPs are frequently deregulated in cancer, less clear is how they exert their pro-tumorigenic effect. Recent data suggest that the E3 ubiquitine ligase activity of IAPs directly influence the assembly of a large death-inducing platform called "ripoptosome"[43] by acting on the stability of the RIP1 kinase. Ripoptosome contains the core components RIP1, FADD and caspase-8 and assembles in response to genotoxic stress-induced depletion of at least two members among XIAP, cIAP1 and cIAP2. Here we show that overexpression of ZFP36 determines the downregulation of XIAP. We believe that this phenomenon somehow mimics genotoxic stress-induced depletion of IAPs and therefore triggers the assembly of the ripoptosome. This hypothesis is supported by an immunoblot showing that casp8, known as the initiator of the extrinsic pathway but now also to be the effector of ripoptosome-triggered necroptotic cell death, is activated in ln827 cells following ZFP36 ectopic expression, and that in the same cells there is an increase of RIP1, that might depend on the fact that this protein is stabilized when the ripoptosome is assembled. In the same cells, we also observed a necrotic cleavage of PARP-1 that further suggests that the ZFP36 induced cell death of ln827 GBM cells could depend on a necroptotic cell death program. Altogether, these data suggest that by restoring the expression of ZFP36, ln827 GBM cells die owing to the activation of two

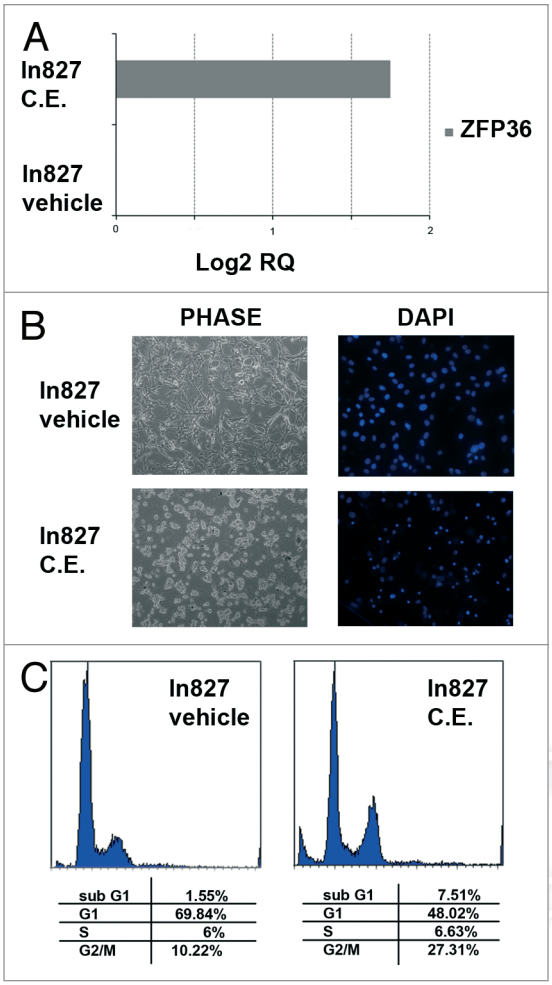

Figure 7. Cinnamon polyphenols treatment of glioma cells induces ZFP36 expression and reduces cells growth. (A) Increase of ZFP36 expression in ln827 was detected by QRT-PCR after 24 h cinnamon polyphenols treatment at the concentration of 0.25 μg/μl. The vehicle-treated sample was used as calibrator for the basal ZFP36 expression levels. (B) Phase contrast images on the left depict the morphology of cinnamon treated glioma at 24 h treatment. Detachment from the vessel is clearly visible in the lower picture. On the right DAPI staining of similarly treated cells shows an increase of the percentage of condensed nuclei. (C) Cell cycle analysis after 24 h of treatment with polyphenols shows the onset of a sub G_1 peak and an increase in the G_2/M phase.

distinct death pathways, the one in which PIM1 and PIM3 are involved and another, which is triggered by XIAP's (and cIAP) depletion. Again, this hypothesis is sustained by the silencing experiments, showing that the inactivation of PIM1, PIM3 and XIAP at once is way more effective in inducing cell death than the single inactivation of the three genes, suggesting that the cumulative effect depends on the activation of different pathways leading to the same biological result, rather than on the interference with a single, common pathway.

Besides the demonstration of new ZFP36 target genes, one of the central findings of this work is that ZFP36 is an element that deserves to be considered for the development of future GBM therapies. In fact, since many difficulties encountered while developing new approaches for GBM depend on its heterogeneity, it could be possible to obtain encouraging results by using chemicals capable of inducing the expression of ZFP36. This hypothesis is sustained by the data shown in the last part of the study, showing the effect of cinnamon polyphenols on GBM cells.

Another finding, although merely speculative, that nevertheless deserves to be underlined, regards the ripoptosome. Although so far it was known that this structure appears in response to genotoxic stress, we provide evidence that it might be assembled also following ZFP36 expression in specific cell contexts, and therefore it might represent not only a phenomenon induced by cytotoxic treatments but it could be a physiological event triggered by specific molecular pathways that surely deserve further investigation.

Materials and Methods

Cell cultures and treatments. The human glioma cell line ln827 was cultured in DMEM medium (Euroclone) supplemented with 10% heat-inactivated fetal bovine serum (Biowhittaker), 2 mM L-glutamine and penicillin/streptomycin (100 μg/ml) (Euroclone). GP + envAm12 cells and human embryonic kidney (HEK) 293 cells were obtained from ATCC and cultured in DMEM medium (Euroclone) supplemented with 10% heat-inactivated fetal bovine serum (Biowhittaker), 1 mM L-glutamine and penicillin/streptomycin (100 μg/ml) (Euroclone). Ecotropic Phoenix cells were cultured in IMDM medium supplemented with 10% heat-inactivated fetal bovine serum, 1 mM L-glutamine and penicillin/streptomycin (100 μg/ml) (Euroclone).

Cinnamon polyphenol extracts were solubilized in DMSO, then added to complete culture medium at the final concentration of 0.25 μg/μl. The medium was not changed until cells were lysed or colonies were scored.

Plasmids and retroviral vectors. Full-length ZFP36 was generated by RT-PCR as already described in reference 27. EcoRI was digested and subsequently cloned within the EcoRI ends of pBABE puro retroviral vector or of pcDNA3.1 expression construct, resulting, respectively, in pBABE ZFP36 and pcDNA3.1 ZFP36 constructs. FlagZFP36 fragment was RT-PCR amplified using FlagZFP36-Direct Primer (DP) (5'-ATG GAC TAC AAA GAT GAC GAC GAC AAG GAT CTG ACT GCC ATC TAC-3') and ZFP36-Reverse Primer (RP) (5'-CGG GCA GTC ACT TTG TCA CT-3'), and the amplified fragments were inserted into the pCR2.1-TOPO T/A cloning vector, from which they were EcoRI excised and cloned into an EcoRI-digested pcDNA3.1 vector.

PIM1, PIM3 and XIAP ARE-containing 3' UTR were amplified by RT-PCR on total RNA extracted from ln827 cells using PIM1 3' UTR-DP (5'-ATG CGC ATT CTA ACC TGG AG-3') and PIM1 3'UTR RP (5'-GAT CTC TTT TAT TCC CCT GTA CAG TAT TT-3'), PIM3 3' UTR-DP (5'-GCA CAC ACA ATG CAA GTC CT-3') and PIM3 3' UTR RP (5'-ACT GAA AGA ACC CCC ATC TG-3'), XIAP 3'UTR DP (5'-TTC ATA GAA CGT CCA GGG TTT A-3') and XIAP 3' UTR RP(5'-GAA

GCT GAG GCA CGA GAA TC-3'). The amplified fragments were then inserted into the pCR2.1-TOPO T/A cloning vector and were fully sequenced. The 3' UTR fragments were then EcoRI excised, blunted and cloned in the sense orientation into a SmaI-digested pGL3-Promoter Vector (Promega) that had previously been modified in order to transfer the multiple cloning region downstream the luciferase reporter gene.

DNA transfection and retroviral infection. Transient transfection of pcDNA3.1-based constructs was performed using Fugene HD reagent (Roche Applied Science) as suggested by the manufacturer's guidelines. The ln827 cell line was transduced using pBABE empty control vector or pBABE ZFP36 retroviral vector. Packaging lines for the pBABE-based constructs were generated by transinfection in the ecotropic Phoenix and successive infection of amphotropic GP + envAm12 cells. Stable packaging cell lines were then produced by 1 μg/ml puromycin selection. Ln827 were transduced by two cycles of infection (6 h each) with viral supernatant in the presence of polybrene (8 μg/ml). Transduced ln827 were selected by mean of one cycle of 0.5 μg/ml puromycin treatment.

Gene silencing. Ln827 cells were treated with Lipofectamine RNAiMAX (Invitrogen) reagent and transfected with a mix of three predesigned siRNAs as per the manufacturer's instructions. PIM1 siRNAs (Hs01_00073783, Hs01_00073785, Hs01_00073786, Sigma Aldrich); PIM3 siRNAs (Hs01_00152603, Hs01_00152604, Hs01_00152605, Sigma Aldrich); XIAP siRNAs (Hs02_00331284, Hs02_00175694, Hs02_00175695, Sigma Aldrich) or control siRNA (Sigma Aldrich). After 18 h, the medium was replaced with complete DMEM medium. Cells were processed 72 h after transfection.

RT-PCR and real-time PCR. Total cellular RNA was extracted using the EuroGOLD Total RNA kit (Euroclone) or RNeasy MicroKit (Qiagen). RNA integrity and concentration was then assessed by the Bio-Analyzer technique (Applied Biosystems).

For RT-PCR, 3 μg of total RNA were reverse transcribed using M-MLV reverse transcriptase (Invitrogen), and then expression of specific genes was assessed by PCR amplification performed using specific primers: GAPDH-DP (5'-GAA GGT GAA GGT CGG AGT C-3'), GAPDH-RP (5'-GAA GGC CAT GCC AGT GAG CT-3'); ZFP36 DP (5'-ATG GAT CTG ACT GCC ATC TAC-3') ZFP36 RP (5'-CGG GCA GTC ACT TTG TCA CT-3'); PIM1 3' UTR-DP (5'-ATG CGC ATT CTA ACC TGG AG-3') and PIM1 3' UTR RP (5'-GAT CTC TTT TAT TCC CCT GTA CAG TAT TT-3'), PIM3 3' UTR-DP (5'-GCA CAC ACA ATG CAA GTC CT-3') and PIM3 3' UTR RP (5'-ACTGAAAGAACCCCCATCTG-3'), XIAP 3' UTR DP (5'-TTC ATA GAA CGT CCA GGG TTT A-3') and XIAP 3' UTR RP (5'-GAA GCT GAG GCA CGA GAA TC-3'). Normalization of the amplified samples was obtained by the glyceraldehydes-3-phosphate dehydrogenase (GAPDH) housekeeping gene.

For quantitative real-time PCR (QRT-PCR) 100 ng of total RNA were reverse-transcribed using the High-Capacity cDNA Archive Kit (Applied Biosystems) according to the manufacturer's instructions; QRT-PCR was then performed with an ABI PRISM 7900 sequence detection system (Applied Biosystems). Primers and probes for the different genes' amplification were provided by Applied Biosystems; quantitation was performed by amplifying GAPDH mRNA as endogenous control.

Antibodies and western blots. Cells were lysed with RIPA buffer containing 50 mM TRIS-HCl (pH 7.4), 150 mM NaCl, 1% NP-40, 1 mM sodium deoxycholate, 1 mM sodium orthovanadate and with added 1 mM EDTA and Complete Protease Inhibitor Cocktail (Roche Applied Science); vortexed for 5 sec; and centrifuged at 16,100 g for 30 min at 4°C. Equal amounts of protein were loaded onto 10–12% SDS-polyacrylamide gel, separated by electrophoresis, and transferred to nitrocellulose membranes (GE Healthcare). Expression of actin was analyzed with a mouse anti-human pan-actin MoAb (Sigma-Aldrich) to normalize protein samples. Membranes were probed with ZFP36 polyclonal antibody (Abcam, ab36558), PIM1 polyclonal antibody (Abcam, ab66767), PIM3 polyclonal antibody (Abcam, ab71321), XIAP (Cell Signaling, #2042), Stat5b (G-2) monoclonal antibody (Santa Cruz Biotechnology, sc-1656), RIP1 mouse monoclonal antibody (BD Transduction Laboratories, 610458), Caspase-8 monoclonal antibody (Cell Signaling, 9746). Blots were then incubated either with anti-rabbit (Cell Signaling, 7074) or anti-mouse (Santa Cruz Biotechnology, sc-2005) IgG-HRP antibodies and detected using BM Chemiluinescence Blotting Substrate (Roche Applied Science).

Immunofluorescence. Briefly, cells cultured on coverslips were fixed with 4% paraformaldehyde for 10 min and permeabilized with 0.1% Triton-X 100/PBS for 3 min. Following incubation with ZFP36 primary antibody, cells were washed and incubated with fluorescently labeled secondary antibody Alexa Fluor® 568 (Invitrogen). Finally, nuclei were counterstained by DAPI (Sigma-Aldrich), and slides were analyzed using a Carl Zeiss Axioskop 40 fluorescent microscope (Carl Zeiss).

Anchorage-independent growth and migration assays. Anchorage-independent growth assays were performed in triplicate in 35 mm well plates. 3 x 10^3 cells per well were seeded in DMEM + 10% FBS containing 0.3% low-melting agarose on the top of the bottom agar containing 0.5% low-melting agarose DMEM + 10% FBS. After 14–21 d colonies were counted. Error bars represent SEM calculated on a set of three to four independent experiments (*$p < 0.05$; **$p < 0.01$). ZFP36 overexpressing cells were first selected by means of puromicyn treatment and then seeded in absence of any selection agent. siRNA transfected ln827 were seeded 72 h after siRNA transfection. For migration assays, cells were cultured at confluence in 24-well plates and then scratched with a thin disposable tip to generate a wound in the cell monolayer. Wound healing was assessed every 24 h by light microscope.

Cell death assays. Apoptotic nuclei were detected by TdT-mediated dUTP terminal nick-end labeling kit (TUNEL) (Roche Applied Science) or by DAPI staining. AnnexinV/PI positivity of indicated cells was assessed by BD PharMingen™ kit (cat. Number 556547). To monitor cell cycle, 1 x 10^5 cells were suspended in 500 μl hypotonic solution (50 μg/ml PI, 0.1% sodium citrate, 0.1% Triton X-100) and then placed at 4°C in the dark for 10 min before flow cytometry analysis.

Luciferase assays. HEK293 cells were plated at a density of 50,000 cells/well 12 h before transfection in 24-well plates. Transfections were carried using Fugene HD reagent (Roche Applied Science). In a typical assay, each well received 200 ng of pGL3-based reporter construct, 200 ng of CMV-b-galactosidase plasmid (Clontech Laboratories) and 10 ng of pcDNA3.1 FlagZfp36, as indicated in figure legends; the difference in total amount of transfected DNA was scaled up with pcDNA3.1 empty vector. After 24 h, cells were harvested. and cell lysates were assayed for luciferase and β-galactosidase activity. Each transfection was done in duplicate in the same experiment, and the plotted luciferase activities represent the average of four different experiments; error bars represent SEM (*$p < 0.05$; **$p < 0.01$).

Preparation of cinnamon extract. Dried cinnamon (*Cinnamomun zeylanicum*) was crushed in a mortar. Five g of powder were then suspended in methanol/water (50/50 v/v; 20 ml) and extracted in ultrasound water bath at room temperature for 30 min. The suspension was centrifuged (4,000 rpm), the supernatant was removed, and the solid was extracted again using the same procedure. Liquid phases were then collected and evaporated in vacuo at room temperature to get rid of methanol and finally subjected to freeze drying. The extract yield was 6.1%. All chemicals were reagent grade and used without further purification; they were purchased from Sigma-Aldrich.

Disclosure of Potential Conflicts of Interest

No potential conflicts of interest were disclosed.

Acknowledgments

T.S. was supported by a Boehringer Ingelheim Fonds travel grant.

References

1. Lai WS, Carballo E, Strum JR, Kennington EA, Phillips RS, Blackshear PJ. Evidence that tristetraprolin binds to AU-rich elements and promotes the deadenylation and destabilization of tumor necrosis factoralpha mRNA. Mol Cell Biol 1999; 19:4311-23; PMID:10330172.
2. Ogilvie RL, Abelson M, Hau HH, Vlasova I, Blackshear PJ, Bohjanen PR. Tristetraprolin downregulates IL-2 gene expression through AU-rich element-mediated mRNA decay. J Immunol 2005; 174:953-61; PMID:15634918.
3. Gomperts M, Corps AN, Pascall JC, Brown KD. Mitogen-induced expression of the primary response gene cMG1 in a rat intestinal epithelial cell-line (RIE-1). FEBS Lett 1992; 306:1-4; PMID:1628738; http://dx.doi.org/10.1016/0014-5793(92)80825-2.
4. Corps AN, Brown KD. Insulin and insulin-like growth factor I stimulate expression of the primary response gene cMG1/TIS11b by a wortmannin-sensitive pathway in RIE-1 cells. FEBS Lett 1995; 368:160-4; PMID:7615073; http://dx.doi.org/10.1016/0014-5793(95)00635-M.
5. Carballo E, Lai WS, Blackshear PJ. Feedback inhibition of macrophage tumor necrosis factoralpha production by tristetraprolin. Science 1998; 281:1001-5; PMID:9703499; http://dx.doi.org/10.1126/science.281.5379.1001.
6. Ciais D, Cherradi N, Bailly S, Grenier E, Berra E, Pouyssegur J, et al. Destabilization of vascular endothelial growth factor mRNA by the zinc-finger protein TIS11b. Oncogene 2004; 23:8673-80; PMID:15467755; http://dx.doi.org/10.1038/sj.onc.1207939.
7. Liang J, Lei T, Song Y, Yanes N, Qi Y, Fu M. RNA-destabilizing factor tristetraprolin negatively regulates NFkappaB signaling. J Biol Chem 2009; 284:29383-90; PMID:19738286; http://dx.doi.org/10.1074/jbc.M109.024745.
8. Kim TW, Yim S, Choi BJ, Jang Y, Lee JJ, Sohn BH, et al. Tristetraprolin regulates the stability of HIF-1alpha mRNA during prolonged hypoxia. Biochem Biophys Res Commun 2010; 391:963-8; PMID:19962963; http://dx.doi.org/10.1016/j.bbrc.2009.11.174.
9. Taylor GA, Thompson MJ, Lai WS, Blackshear PJ. Phosphorylation of tristetraprolin, a potential zinc finger transcription factor, by mitogen stimulation in intact cells and by mitogen-activated protein kinase in vitro. J Biol Chem 1995; 270:13341-7; PMID:7768935; http://dx.doi.org/10.1074/jbc.270.22.13341.
10. Carballo E, Cao H, Lai WS, Kennington EA, Campbell D, Blackshear PJ. Decreased sensitivity of tristetraprolin-deficient cells to p38 inhibitors suggests the involvement of tristetraprolin in the p38 signaling pathway. J Biol Chem 2001; 276:42580-7; PMID:11546803; http://dx.doi.org/10.1074/jbc.M104953200.
11. Mahtani KR, Brook M, Dean JL, Sully G, Saklatvala J, Clark AR. Mitogen-activated protein kinase p38 controls the expression and posttranslational modification of tristetraprolin, a regulator of tumor necrosis factoralpha mRNA stability. Mol Cell Biol 2001; 21:6461-9; PMID:11533235; http://dx.doi.org/10.1128/MCB.21.9.6461-9.2001.
12. Johnson BA, Geha M, Blackwell TK. Similar but distinct effects of the tristetraprolin/TIS11 immediate-early proteins on cell survival. Oncogene 2000; 19:1657-64; PMID:10763822; http://dx.doi.org/10.1038/sj.onc.1203474.
13. Johnson BA, Blackwell TK. Multiple tristetraprolin sequence domains required to induce apoptosis and modulate responses to TNFalpha through distinct pathways. Oncogene 2002; 21:4237-46; PMID:12082611; http://dx.doi.org/10.1038/sj.onc.1205526.
14. Amit I, Citri A, Shay T, Lu Y, Katz M, Zhang F, et al. A module of negative feedback regulators defines growth factor signaling. Nat Genet 2007; 39:503-12; PMID:17322878; http://dx.doi.org/10.1038/ng1987.
15. Schichl YM, Resch U, Hofer-Warbinek R, de Martin R. Tristetraprolin impairs NFkappaB/p65 nuclear translocation. J Biol Chem 2009; 284:29571-81; PMID:19654331; http://dx.doi.org/10.1074/jbc.M109.031237.
16. Brennan SE, Kuwano Y, Alkharouf N, Blackshear PJ, Gorospe M, Wilson GM. The mRNA-destabilizing protein tristetraprolin is suppressed in many cancers, altering tumorigenic phenotypes and patient prognosis. Cancer Res 2009; 69:5168-76; PMID:19491267; http://dx.doi.org/10.1158/0008-5472.CAN-08-4238.
17. Suswam E, Li Y, Zhang X, Gillespie GY, Li X, Shacka JJ, et al. Tristetraprolin downregulates interleukin-8 and vascular endothelial growth factor in malignant glioma cells. Cancer Res 2008; 68:674-82; PMID:18245466; http://dx.doi.org/10.1158/0008-5472.CAN-07-2751.
18. Krakstad C, Chekenya M. Survival signalling and apoptosis resistance in glioblastomas: opportunities for targeted therapeutics. Mol Cancer 2010; 9:135; PMID:20515495; http://dx.doi.org/10.1186/1476-4598-9-135.
19. Frederick L, Wang XY, Eley G, James CD. Diversity and frequency of epidermal growth factor receptor mutations in human glioblastomas. Cancer Res 2000; 60:1383-7; PMID:10728703.
20. Senft C, Polacin M, Priester M, Seifert V, Kögel D, Weissenberger J. The nontoxic natural compound Curcumin exerts anti-proliferative, anti-migratory and anti-invasive properties against malignant gliomas. BMC Cancer 2010; 10:491; PMID:20840775; http://dx.doi.org/10.1186/1471-2407-10-491.
21. Raychaudhuri B, Vogelbaum MA. IL-8 is a mediator of NFκB induced invasion by gliomas. J Neurooncol 2011; 101:227-35; PMID:20577780; http://dx.doi.org/10.1007/s11060-010-0261-2.
22. Xie TX, Xia Z, Zhang N, Gong W, Huang S. Constitutive NFkappaB activity regulates the expression of VEGF and IL-8 and tumor angiogenesis of human glioblastoma. Oncol Rep 2010; 23:725-32; PMID:20127012.
23. Joo KM, Kim SY, Jin X, Song SY, Kong DS, Lee JI, et al. Clinical and biological implications of CD133-positive and CD133-negative cells in glioblastomas. Lab Invest 2008; 88:808-15; PMID:18560366; http://dx.doi.org/10.1038/labinvest.2008.57.
24. Siegelin MD, Gaiser T, Siegelin Y. The XIAP inhibitor Embelin enhances TRAIL-mediated apoptosis in malignant glioma cells by downregulation of the short isoform of FLIP. Neurochem Int 2009; 55:423-30; PMID:19409438; http://dx.doi.org/10.1016/j.neuint.2009.04.011.
25. Vellanki SHK, Grabrucker A, Liebau S, Proepper C, Eramo A, Braun V, et al. Small-molecule XIAP inhibitors enhance gamma-irradiation-induced apoptosis in glioblastoma. Neoplasia 2009; 11:743-52; PMID:19649204.
26. Tenev T, Bianchi K, Darding M, Broemer M, Langlais C, Wallberg F, et al. The Ripoptosome, a signaling platform that assembles in response to genotoxic stress and loss of IAPs. Mol Cell 2011; 43:432-48; PMID:21737329; http://dx.doi.org/10.1016/j.molcel.2011.06.006.
27. Vignudelli T, Selmi T, Martello A, Parenti S, Grande A, Gemelli C, et al. ZFP36L1 negatively regulates erythroid differentiation of $CD34^+$ hematopoietic stem cells by interfering with the Stat5b pathway. Mol Biol Cell 2010; 21:3340-51; PMID:20702587; http://dx.doi.org/10.1091/mbc.E10-01-0040.
28. Gobeil S, Boucher CC, Nadeau D, Poirier GG. Characterization of the necrotic cleavage of poly(ADP-ribose) polymerase (PARP-1): implication of lysosomal proteases. Cell Death Differ 2001; 8:588-94; PMID:11536009; http://dx.doi.org/10.1038/sj.cdd.4400851.
29. Liang QC, Xiong H, Zhao ZW, Jia D, Li WX, Qin HZ, et al. Inhibition of transcription factor STAT5b suppresses proliferation, induces G_1 cell cycle arrest and reduces tumor cell invasion in human glioblastoma multiforme cells. Cancer Lett 2009; 273:164-71; PMID:18793823; http://dx.doi.org/10.1016/j.canlet.2008.08.011.
30. Chang M, Kanwar N, Feng E, Siu A, Liu X, Ma D, et al. PIM kinase inhibitors downregulate STAT3 (Tyr705) phosphorylation. Mol Cancer Ther 2010; 9:2478-87; PMID:20667852; http://dx.doi.org/10.1158/1535-7163.MCT-10-0321.
31. Senft C, Priester M, Polacin M, Schröder K, Seifert V, Kögel D, et al. Inhibition of the JAK-2/STAT3 signaling pathway impedes the migratory and invasive potential of human glioblastoma cells. J Neurooncol 2011; 101:393-403; PMID:20589525; http://dx.doi.org/10.1007/s11060-010-0273-y.

32. Lindemann C, Hackmann O, Delic S, Schmidt N, Reifenberger G, Riemenschneider MJ. SOCS3 promoter methylation is mutually exclusive to EGFR amplification in gliomas and promotes glioma cell invasion through STAT3 and FAK activation. Acta Neuropathol 2011; 122:241-51; PMID:21590492; http://dx.doi.org/10.1007/s00401-011-0832-0.
33. Cao H, Anderson RA. Cinnamon polyphenol extract regulates tristetraprolin and related gene expression in mouse adipocytes. J Agric Food Chem 2011; 59:2739-44; PMID:21329350; http://dx.doi.org/10.1021/jf103527x.
34. Griseri P, Bourcier C, Hieblot C, Essafi-Benkhadir K, Chamorey E, Touriol C, et al. A synonymous polymorphism of the Tristetraprolin (TTP) gene, an AU-rich mRNA-binding protein, affects translation efficiency and response to Herceptin treatment in breast cancer patients. Hum Mol Genet 2011; 20:4556-68; PMID:21875902; http://dx.doi.org/10.1093/hmg/ddr390.
35. Cha HJ, Lee HH, Chae SW, Cho WJ, Kim YM, Choi HJ, et al. Tristetraprolin downregulates the expression of both VEGF and COX-2 in human colon cancer. Hepatogastroenterology 2011; 58:790-5; PMID:21830391.
36. Sanduja S, Kaza V, Dixon DA. The mRNA decay factor tristetraprolin (TTP) induces senescence in human papillomavirus-transformed cervical cancer cells by targeting E6-AP ubiquitin ligase. Aging (Albany NY) 2009; 1:803-17; PMID:20157568.
37. Baou M, Jewell A, Muthurania A, Wickremasinghe RG, Yong KL, Carr R, et al. Involvement of Tis11b, an AU-rich binding protein, in induction of apoptosis by rituximab in B cell chronic lymphocytic leukemia cells. Leukemia 2009; 23:986-9; PMID:19092855; http://dx.doi.org/10.1038/leu.2008.340.
38. Brault L, Gasser C, Bracher F, Huber K, Knapp S, Schwaller J. PIM serine/threonine kinases in the pathogenesis and therapy of hematologic malignancies and solid cancers. Haematologica 2010; 95:1004-15; PMID:20145274; http://dx.doi.org/10.3324/haematol.2009.017079.
39. Mukaida N, Wang YY, Li YY. Roles of Pim-3, a novel survival kinase, in tumorigenesis. Cancer Sci 2011; 102:1437-42; PMID:21518143; http://dx.doi.org/10.1111/j.1349-7006.2011.01966.x.
40. Hu XF, Li J, Vandervalk S, Wang Z, Magnuson NS, Xing PX. PIM-1-specific mAb suppresses human and mouse tumor growth by decreasing PIM-1 levels, reducing Akt phosphorylation and activating apoptosis. J Clin Invest 2009; 119:362-75; PMID:19147983.
41. Santio NM, Vahakoski RL, Rainio EM, Sandholm JA, Virtanen SS, Prudhomme M, et al. Pim-selective inhibitor DHPCC-9 reveals Pim kinases as potent stimulators of cancer cell migration and invasion. Mol Cancer 2010; 9:279; PMID:20958956; http://dx.doi.org/10.1186/1476-4598-9-279.
42. Kim CW, Kim HK, Vo MT, et al. Tristetraprolin controls the stability of cIAP2 mRNA through binding to the 3' UTR of cIAP2 mRNA. Biochem Biophys Res Commun 2010; 10:46-52; http://dx.doi.org/10.1016/j.bbrc.2010.07.136.
43. Darding M, Meier P. IAPs: guardians of RIPK1. Cell Death Differ 2012; 19:58-66; PMID:22095281; http://dx.doi.org/10.1038/cdd.2011.163.